Omni-Akuatika, 22 (1): 27 - 39, 2026
ISSN: 1858-3873 print / 2476-9347 online

Research Article

journal homepage: http://ojs.omniakuatika.net

Spatial and Temporal Influences of El-Niño Southern Oscillation and Indian Ocean Dipole on Natuna Sea Surface Temperature and Surrounding Areas

Alextansius Verel Renaldo*, **Arie Antasari Kushadiwijayanto, Apriansyah**

Department of Marine Science, Faculty of Mathematics and Natural Sciences, Tanjungpura University, Jl. Prof.Dr.H.Hadari Nawawi, Pontianak, 78124 Indonesia

**Corresponding author: alextansius@gmail.com*

Received 14 January 2025; Revised 27 May 2026, Accepted 28 May 2026; Available online 18 August 2026, Published 18 August 2026

ABSTRACT

This study aims to investigate the spatial and temporal impacts of El Niño-Southern Oscillation (ENSO) and Indian Ocean Dipole (IOD) on Sea Surface Temperature (SST) variations in the Natuna Sea and its adjacent waters. In this study, Cross Wavelet Transform (XWT) and Partial Correlation were used to determine the time-frequency relationship and isolate the specific influence of ENSO and IOD on SST. These primary methods were substantiated by Time Series Analysis, Power Spectral Density (PSD), and Cross Correlation, which first identified the dominant interannual periodicities and lag phases required for causal analysis. Analysis reveals that the interannual phenomenon (in a period of 2-7 years) is dominant in controlling the SST anomalies in the Natuna Sea. The XWT analysis shows that SST responds to ENSO and IOD within a 2-7 year band, though with varying lag phases of 2-3 months in the northern region and 7-10 months in the southern region. Meanwhile Partial Correlation analysis confirms a positive relationship across the basin with the IOD exhibiting a stronger and more uniform influence (r = 0.5-0.8) compared to ENSO (r = 0.1-0.7). These results suggest that SST warming in the Natuna Sea is driven primarily by atmospheric teleconnections rather than direct oceanic advection, particularly in the northern region.

Keywords: El Niño-Southern Oscillation, Indian Ocean Dipole, SST, Cross Wavelet Transform, Partial Correlation

ABSTRAK

Penelitian ini bertujuan untuk mengetahui dampak spasial dan temporal *El Niño-Southern Oscillation* (ENSO) and *Indian Ocean Dipole* (IOD) terhadap variasi SPL di Laut Natuna dan perairan sekitarnya. Dalam penelitian ini digunakan metodologi seperti *Cross Wavelet Transform* (XWT) and Korelasi Parsial digunakan untuk menentukan hubungan waktu-frekuensi dan mengisolasi pengaruh spesifik dari ENSO dan IOD terhadap anomali SPL. Metode-metode utama ini didukung oleh analisis *time-series, Power Spectral Density* (PSD), dan analisis *cross-correlation* untuk mengidentifikasi periodisitas antartahunan yang dominan dan fase jeda (*lag phase*). Hasil penelitian menunjukkan bahwa periodisitas antartahunan dalam rentang waktu 2-7 tahun mengendalikan anomali SPL di Laut Natuna secara dominan. Analisis XWT menunjukkan bahwa SPL merespon ENSO and IOD dalam rentang waktu 2-7 tahun, meskipun dengan kekuatan dan fase jeda yang bervariasi selama 2-3 bulan di wilayah utara dan 7-10 bulan di wilayah selatan. Sementara itu, analisis Korelasi Parsial menunjukkan adanya hubungan positif yang luas di seluruh cekungan, di mana IOD menunjukkan pengaruh yang lebih kuat dan seragam (r = 0,5-0,8) dibandingkan dengan ENSO (r = 0,1-0,7). Temuan ini menunjukkan bahwa pemanasan SPL di Laut Natuna terutama didorong oleh telekoneksi atmosfer dibandingkan dengan adveksi laut langsung, khususnya di wilayah utara.

Kata kunci: El Niño-Southern Oscillation, Indian Ocean Dipole, SPL, Cross Wavelet Transform (XWT), Korelasi Parsial

http://dx.doi.org/10.20884/1.oa.2026.22.1.1236

1. Introduction

Indonesian waters is a complex region where local climate variability is strongly affected by the interactions between the Pacific and Indian Ocean as its adjacent ocean. Two primary interannual climate phenomena, the El Niño-Southern Oscillation (ENSO) happening in the Pacific and the Indian Ocean Dipole (IOD) happening in the Indian Ocean play a significant role by disrupting the atmospheric and oceanic circulation over this region (Can, 1983; Saji et al., 1999; Webster et al., 1999). The Natuna Sea functions as a critical shallow water exchange pathway between the South China Sea and the Java Sea is notably sensitive to these atmospheric shifts (Al-Fiah & Burhanuddin, 2023). Changes in Sea Surface Temperature (SST) within this region are critical indicators of these climatic disruptions, yet the precise timing and magnitude of its response to remote forcings vary spatially. Previous studies have established that ENSO and IOD influence remote oceans through an ‘atmospheric bridge’ where changes in Walker Circulation modify local wind stress, cloud cover and evaporation (Klein et al., 1999; Alexander et al., 2002). This atmospheric transmission process inherently creates a time delay or ‘lag phase’ between the peak of open ocean climate indices like Oceanic Niño Index (ONI) and Dipole Mode Index (DMI) towards the subsequent SST response in the semi enclosed Natuna Sea (Lanzante, 1996; Curtis & Hastenrath, 1995). While the shifts in the Walker Circulation and changes in wind stress are the general mechanism of these events (Wang, 2002; Klein et al., 1999), the regional response is often distorted by seasonal monsoonal patterns and localized circulation (Wang et al., 2006; Zhu et al., 2003). Understanding this temporal lag is important to predict how regional fisheries and weather patterns will react to developing climate anomalies.

Despite the well documented general correlations between these climate indices and Indonesian SST, the specific time-frequency localization and the independent influence of ENSO and IOD remain under explored in the Natuna Sea. Previous studies have often analyzed these events together or relied on linear correlations. Therefore, there is a chance to overlook the non-stationary/fluctuating nature of climate signals (Isa et al., 2020). This creates an important knowledge gap, since it becomes difficult to determine which phenomenon employs the dominant causal forcing and at what time delay when both ENSO and IOD are active simultaneously.

Therefore, this study aims to clarify the hydro-climatological dynamics of the Natuna Sea and its surrounding areas by addressing these gaps. Specifically, this research utilizes Cross-Wavelet Transform (XWT) to determine the precise time-lag response and coherent periodicity of SST to climate indices (Torrence & Compo, 1998; Grinsted, 2024). Furthermore, Partial Correlation analysis is employed to isolate the individual influence of ENSO and IOD, removing the confounding effects of their co-occurrence (Pearson, 1900). By integrating these methods, this study provides a quantitative assessment of how multiscale climate variability regulates regional ocean temperatures.

2. Materials and methods

2.1 Research Map

This research was conducted within the study area of the Natuna Sea and its surrounding waters (see Figure 1), which was located by coordinates 7°8'0"N to 4°6'0"S and 102°0'0"E to 111°0'0"E. Following the division established by Pratama et al. (2023), two distinct sub-regions were utilized based on the environmental characteristics of the region. The Northern Natuna Sea (further referred to as the Northern Region) was dynamically controlled by seasonal oceanic current circulation and eddy formation, whereas the Southern Natuna Sea / Karimata Strait (further referred to as the Southern Region) was primarily influenced by terrestrial river runoff and nutrient discharge. Therefore, the area was geographically divided by the equator into the Northern Region (above the equator) and the Southern Region (below the equator).

2.2 Data Processing

A dual scale approach was used in this study, where Cross Wavelet Transform (XWT) is applied to the spatially averaged time series of each sub-region to resolve the temporal frequency and phase relationship, while Partial Correlation analysis was applied to the entire spatial SST field to map the regional distribution of ENSO and IOD influences. The three supporting methods namely Time Series Analysis, Power Spectral Density (PSD), and Cross Correlation were used to support the temporal signal analysis. The SST data used consisted of secondary data that could be downloaded through the CMEMS website while Oceanic Niño Index (ONI) and Dipole Mode Index (DMI) data can be accessed on the NOAA website (Table 3). To ensure rigorous event classification, the ONI data were stratified by strictly following the standard NOAA guidelines while DMI data followed the thresholds established by Saji et al. (1999). Specifically El Niño and La Niña events were defined by monthly ONI anomalies exceeding +0.5℃ and -0.5℃, respectively sustained for a minimum of five consecutive months, following the operational definitions by the Climate Prediction Center (NOAA-CPC, 2015; L'Heureux et al., 2017). Simultaneously, IOD+ and IOD- events were classified based on the standard threshold of +0.4℃ and -0.4℃, respectively, to capture distinct dipole modes (Saji et al., 1999). To ensure computational accuracy, eliminate human error, and maintain a strict scientific reproducibility, this entire stratification and event matching process was fully executed and automated through a script-based approach in MATLAB.

Before the temporal analysis, the four dimensional SST spatial data (longitude, latitude, depth, time) were converted into a one dimensional time series for each respective region. This was done by calculating the spatial average of all valid grid points within the Northern and Southern boundaries for each time step (month), which shown by the following equation:

$$\underline{SST}(t) = \frac{1}{N}\sum_{i=1}^{N} SST_i(t) \text{.....................(1)}$$

Where, $\underline{SST}(t)$ = Spatially averaged SST at time t. N = Total number of valid oceanic grid points within the specific sub-region. $SST_i(t)$ = Temperature value at the i-th grid point

Once the regional time series were established, the data were converted into Sea Surface Temperature Anomalies by subtracting the long term monthly climatological means to eliminate the dominant annual cycle. Following this, a fourth order Butterworth bandpass filter was applied with cut off frequencies corresponding to periods of 2 years (high frequency cut off) and 7 years (low frequency cut off). This filtering step is done to remove high frequency seasonal noise and long-term decadal trends to ensure that the analysis focused strictly on the interannual variability relevant to both ENSO and IOD dynamics.

2.3 Time Series and Power Spectral Density

Time Series analysis was conducted for all data to identify the fluctuation patterns that occurred in SST, ONI, and DMI. The Time Series analysis was also completed with linear regression analysis to review the trends of each variable. Then, PSD analysis of SST was conducted to identify dominant periodicities with a specific focus on detecting significant spectral energy in the interannual band (2-7 years) to confirm the influence of ENSO and IOD on SST fluctuations in the Natuna Sea. The PSD analysis was executed using the Welch method available in the MATLAB software.

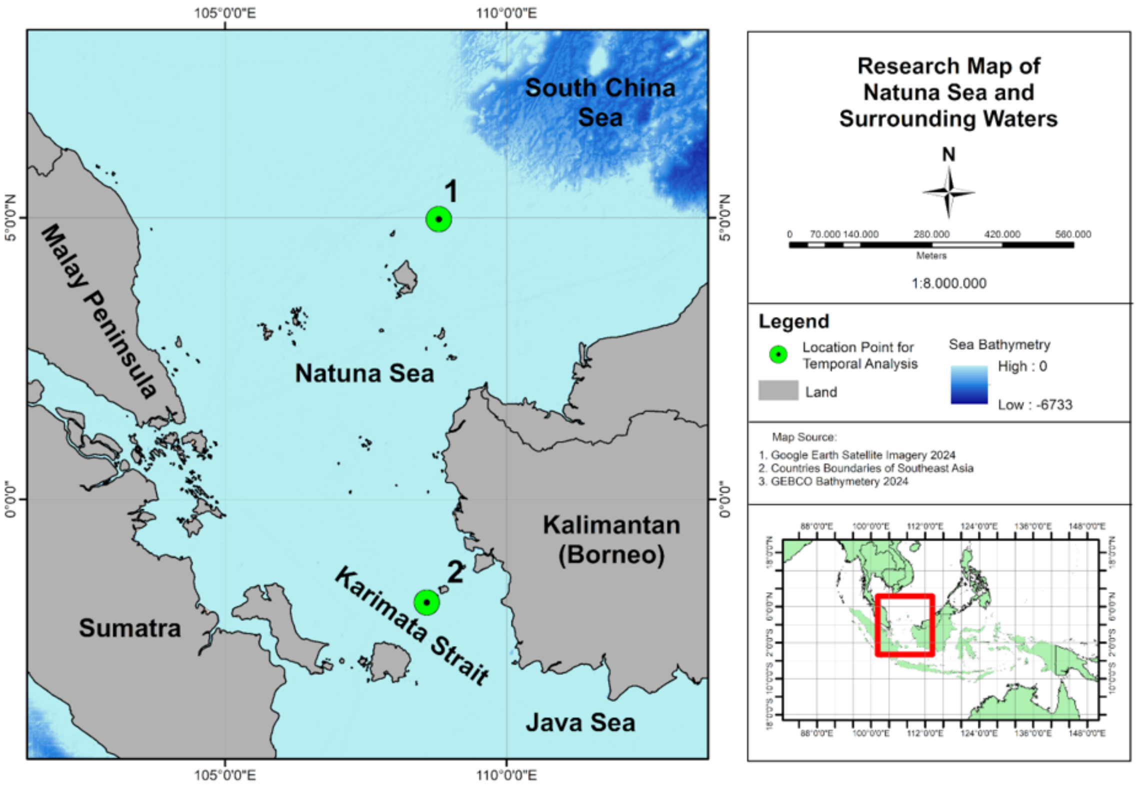

Figure 1. Research Map

2.4 Cross Wavelet Transform (XWT) and Cross Correlation

Temporal signal analysis was performed using the XWT to identify the probability of a relationship between two time series that varied simultaneously and to quantify the strength and direction of the relationship between the variables. The XWT analysis was implented using a toolbox that can be downloaded at https://www.mathworks.com/matlabcentral/fileexchange/47985-cross-wavelet-and-wavelet-coherence (Grinsted, 2024). Cross correlation analysis was then used to examine and pinpoint the exact peak signal and lag between SST and ONI/DMI. The optimal lag was defined as the time delay corresponding to the maximum correlation coefficient. Simultaneously, these methods were used to identify the dominant frequency periods and phase shifts in the time-frequency dimension. The phase shift identified at the representative regions was applied as a uniform time delay across the entire spatial domain for the subsequent Partial Correlation analysis in order to ensure that the spatial maps reflect the region's response at the climate signal's peak.

The theoretical distribution of the cross-wavelet power of two time series with background power spectra P_k^X and P_k^Y was defined by Torrence and Compo (1998) as:

$$D\left(\frac{|W_n^X(s)W_n^{Y*}(s)|}{\sigma_X\sigma_Y} < p\right) = \frac{Z_v(p)}{v}\sqrt{P_k^X P_k^Y} \quad \text{.............(2)}$$

Where $Z_v(p)$ is the confidence level associated with the probability p for a pdf defined by the square root of the product of two χ^2 distributions

2.5 Partial Correlation

Partial Correlation Analysis was then conducted across the entire spatial domain, integrating the lag values obtained from the XWT and Cross Correlation Methods. This allowed for the visualization of the spatial distribution of the relationship intensity between SST and ENSO/IOD across the whole Natuna Sea, rather than just on isolated points. Conceptually, standard linear correlation can give misleading results when analyzing ENSO and IOD because these two climate modes often co-occur and interact. In order to address this multicollinearity, Partial Correlation was essential to statistically isolate the unique contribution of each variable (e.g. ENSO) while removing the confounding influence of the other (e.g. IOD).

A single correlation calculation is required before performing a partial correlation calculation. The single correlation equation was expressed as follows (Pearson, 1895):

$$r = \frac{n\sqrt{xy}-(\sum x)(\sum y)}{\sqrt{(n\sum x^2-(\sum x)^2)(n\sum y^2-(\sum y)^2)}} \quad \text{......................... (3)}$$

Using the single correlation values, the partial correlation calculation was then executed using this following equation:

$$r_{y.x1-x2} = \frac{r_{yx1} - r_{yx2}r_{x1x2}}{\sqrt{1-r_{x1x2}^2}\sqrt{1-r_{yx2}^2}} \quad \text{...................... (4)}$$

Where, $r_{y.x1-x2}$ = Partial Correlation coefficient between SST and the primary index (x_1) with the influence of the secondary index removed (x_2). y = SST, x_1= Primary climate index (ONI or DMI), x_2 = Secondary/Control climate index (DMI or ONI).

Correlation score categories are shown in the following table (see Table 1). Matlab functions used and data sources are shown below (see Table 2 and Table 3).

Table 1. Correlation Coefficient Interpretation based on Guilford (1956)

Coefficient Interval	Level of Correlation
0,000-0,199	Very Weak
0,200-0,399	Weak
0,400-0,599	Moderate
0,600-0,799	Strong
0,800-1,000	Very Strong

Table 2. Matlab Function Used

No.	*Method*	*MATLAB Function*
1	SST filter	butter
2	Time Series	plot polyfit polyval
3	Power Spectral Density	pwelch
4	Cross Wavelet Transform	xwt
5	Cross Correlation	xcorr
6	Partial Correlation	partialcorr

3. Results and Discussion

3.1. Time Series and Power Spectral Density Analysis

The time series results in Figure 2 show in general that there is an interannual pattern that occurs in SST in the Natuna Sea. The results also show that the SST signal tends to be in phase with the index (SST crest/trough) occur when Oscillation Nino Index (ONI) and Dipole Mode Index (DMI) crest/trough)), and are clearly visible in 1997-1998 and 2015-2016. From the linear regression results in Table 4, the SST slope of 0.0012566°C indicates that SST tends to increase at a rate of 0.015079°C/year over the study period. While a detailed trend attribution is beyond the scope of this study, this observed warming rate is consistent with the rapid warming of the South China Sea Large Marine Ecosystem documented by Belkin (2009) and Liu and Zhang (2013) which range from 0.014°C/year to 0.016°C/year during recent decades. On the contrary, the trends observed in the ONI and DMI indices are negligible since they are consistent with their nature as oscillating climate modes.

3.2. Cross Wavelet Transform and Cross Correlation Analysis

The XWT results between SST and ONI at North and South Region that can be seen in Figure 4 show a strong influence on SST anomalies within the 2 to 7 year band, which refers to an interannual phenomenon. Significant cross wavelet power was observed with spectral density values reaching magnitudes of 3-5 (variance units) at Northern Region, peaking during the extreme events in 1997-1999 and 2015. Similarly, the spectral density values in Southern Region reaching magnitudes of 3-4 during 1997-1999 and 2011-2016. These values indicate strong common variance between the SST anomalies and climate index during these periods. These values correspond to the El Niño index peaks in 1997 (ONI = 2.4) and 2015 (ONI = 2.6), and La Niña peaks in 1999 (ONI = -1.7) and 2011 (ONI = -1.6). The phase relationship, which is indicated by the direction of the arrows, reveals diverse regional responses. The Northern Region is dominated by rightward pointing arrows, indicating an in-phase relationship. This means positive ONI anomalies (El Nino) are associated with the warming of the SST. On the contrary, the Southern Region is dominated by upward pointing arrows which indicates that ONI leads SST by approximately 90° (quarter cycle). This phase difference suggests a delayed response in the southern region compared to the north.

The phase relationship between ONI and SST varies significantly across the frequency bands which reflects different physical response mechanisms. At the North Region, the high frequency band (around 2 year band) shows a 90° phase lag, indicated by upward pointing arrows. This indicates that SST responds to ENSO fluctuations with a distinct delay. However, within the dominant interannual band (3-6 year band, particularly 1999-2009) the relationship shifts to be enormously in-phase (rightward pointing arrows). This suggests a more direct and immediate teleconnection during major ENSO events.

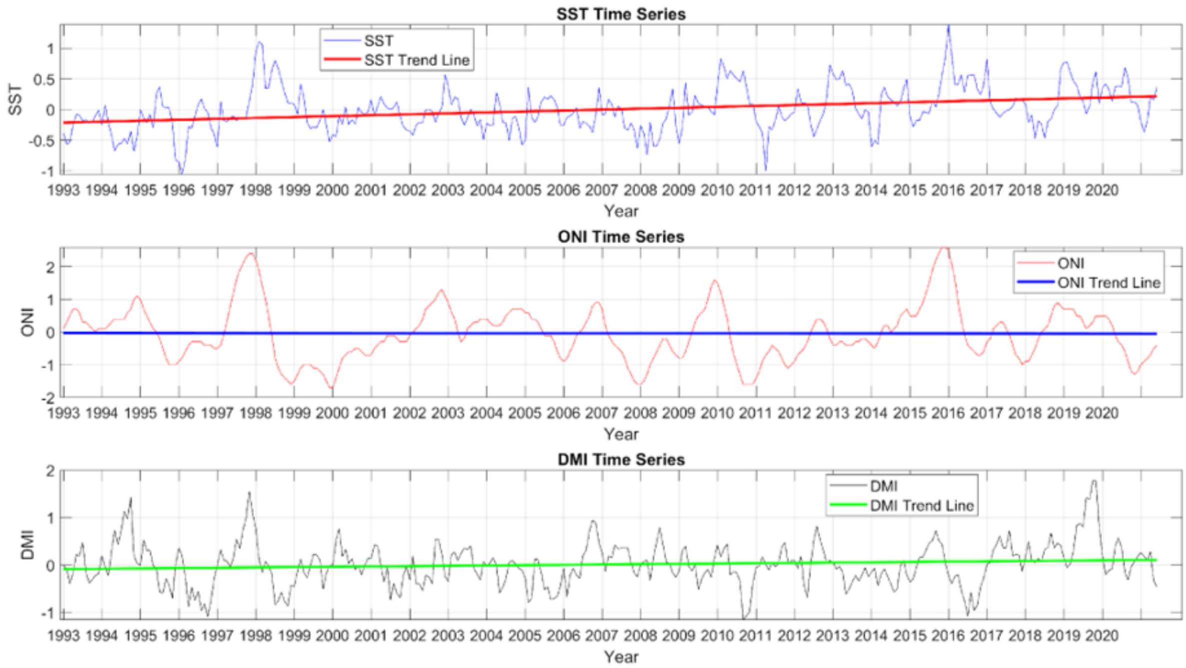

Figure 2. Time series of SST (a) ONI (b) and DMI (c)

Table 3. Data Source

No.	Data	Data Source	Data Specifications		Data Period	References
			Spatial Resolution	Temporal Resolution		
1	Sea Surface Temperature	CMEMS	0,083°	Monthly	1993-2021	https://data.marine.copernicus.eu/product/GLOBAL_MULTIYEAR_PHY_001_030/download
2	ENSO Indices (ONI)	NOAA		Monthly	1993-2021	https://origin.cpc.ncep.noaa.gov/products/analysis_monitoring/ensostuff/ONI_v5.php
3	IOD Indices (DMI)	NOAA		Monthly	1993-2021	https://www.cpc.ncep.noaa.gov/products/international/Ocean_monitoring/IODMI/DMI_month.html

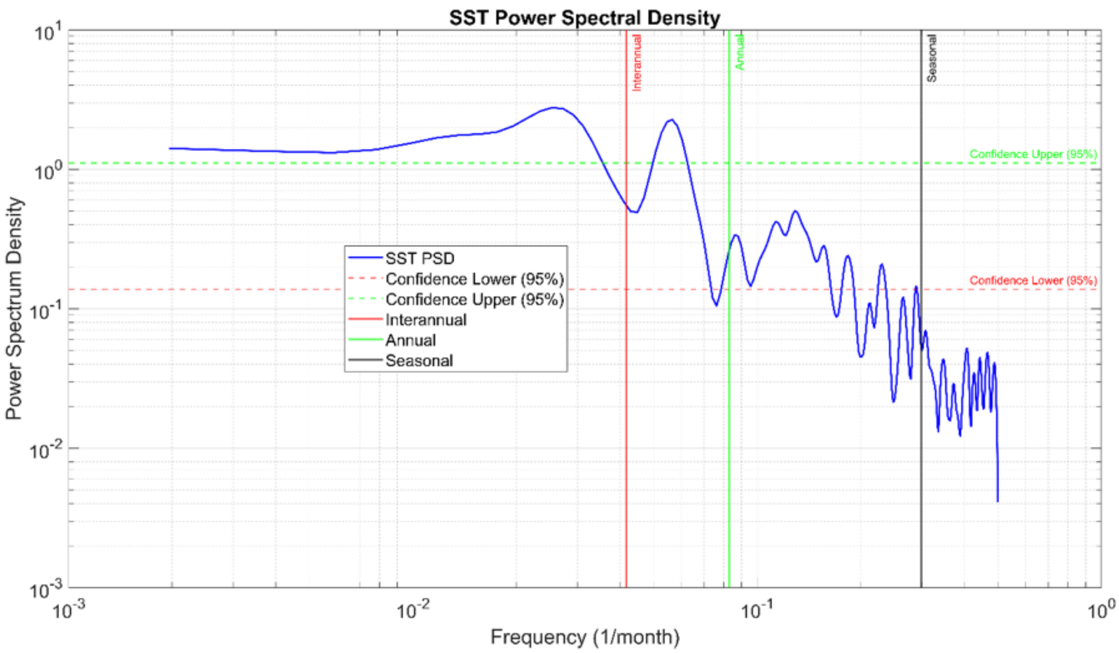

Figure 3. Power Spectral Density of SST in Natuna Sea

Table 4. Slope and Trend of SST, ONI, and DMI

Variable	Slope/month	Trend/year (°C)
SST	0.0012566	0.015079
ONI	-0.000070438	-0.00084525
DMI	0.00056379	0.0067655

In contrast to the North, the Southern Region shows a consistent slower response. The <3 year band is characterized by northwest pointing arrows, showing phase lags of 90°-135°. This indicates that the index leads SST significantly. Even in the 3-6 year band, while in-phase behaviour was observed during 1999-2011, the signal transitions to a 45°-90° lag, indicated by northeast pointing arrows in the later years. These spectral findings are corroborated by the Cross Correlation analysis which identified the maximum correlation at a lag of +3 months for the Northern Region (r = 0.4425) and +7 months for the Southern Region (r = 0.5097). This confirms a propagation delay which indicates that the ENSO signal influences the Southern Natuna Sea/Karimata Strait approximately 4 months later than the North.

The XWT results between SST and DMI at Northern Region and Southern Region in Figure 5 show a strong influence on SST anomalies in the 2-7 year band. Similar to the ENSO results, significant cross wavelet power was also observed at both regions, with intensity levels reaching magnitudes 3-5. These high power regions are most prominent during the IOD events in 1997-1999 and 2013-2016. This confirms that IOD events drive a substantial variance in the region's thermal structure.

The phase relationship reveals a complex spatial contrast. At the Northern Region, the DMI signal is generally weak and inconsistent. In the <3 year period band (1997-2001), upward pointing arrows indicate that DMI leads SST by 90°. However, in the 3-6 year band (1997-2008), the phase shifts to downward pointing arrows. This implies an inverse lead relationship where SST appears to go before the index or indicating an unstable phase locking. This instability is reflected in the Cross Correlation analysis where a very weak maximum correlation was found (r = 0.1995) at a short lag of +2 months. This may suggest that the IOD has a negligible direct influence on the Northern Natuna Sea.

In contrast to the North, the Southern Region shows a much stronger and more delayed response. The <3 year band is dominated by northwest pointing arows (phase lag ≈ 135°). This indicates that the DMI leads SST with a significant delay and a shift toward anti-phase behaviour. This is consistent with the Cross Correlation results which shows a strong maximum correlation (r = 0.7777) at a great lag of +10 months. This indicates a distinct spatial variability in response times with the Northern Region responding approximately 8 months earlier than the South. This delay suggests that the Southern Region (Southern Natuna Sea/Karimata Strait) exhibits a slower temperature response to remote climate forcing compared to the open Northern boundary.

3.3. Partial Correlation

Partial correlation analysis was used to evaluate the impact of ENSO and IOD on SST by eliminating the influence of other interconnected variables. The statistical significance of the partial correlations was assessed using a t-test at the 95% confidence level (α = 0.05). Areas with statistically significant correlation (ρ < 0.05) are marked with black dots in the spatial maps (see Figure 6). A lag of 7 months was selected based on the XWT and Cross Correlation analysis, which showed the highest correlation in that range.

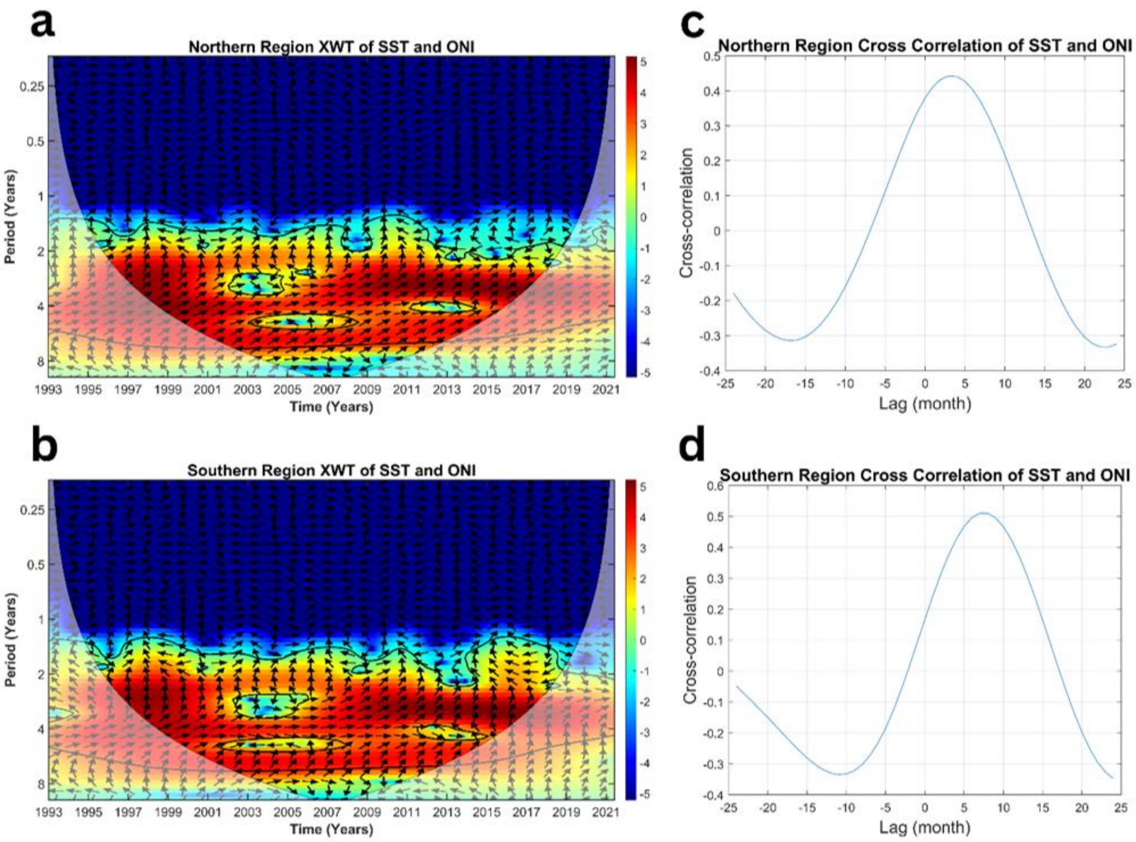

Figure 4. XWT of SST and ONI on Northern Region (a), Southern Region (b) and Cross Correlation of SST and ONI on Northern Region (c) Southern Region (d)

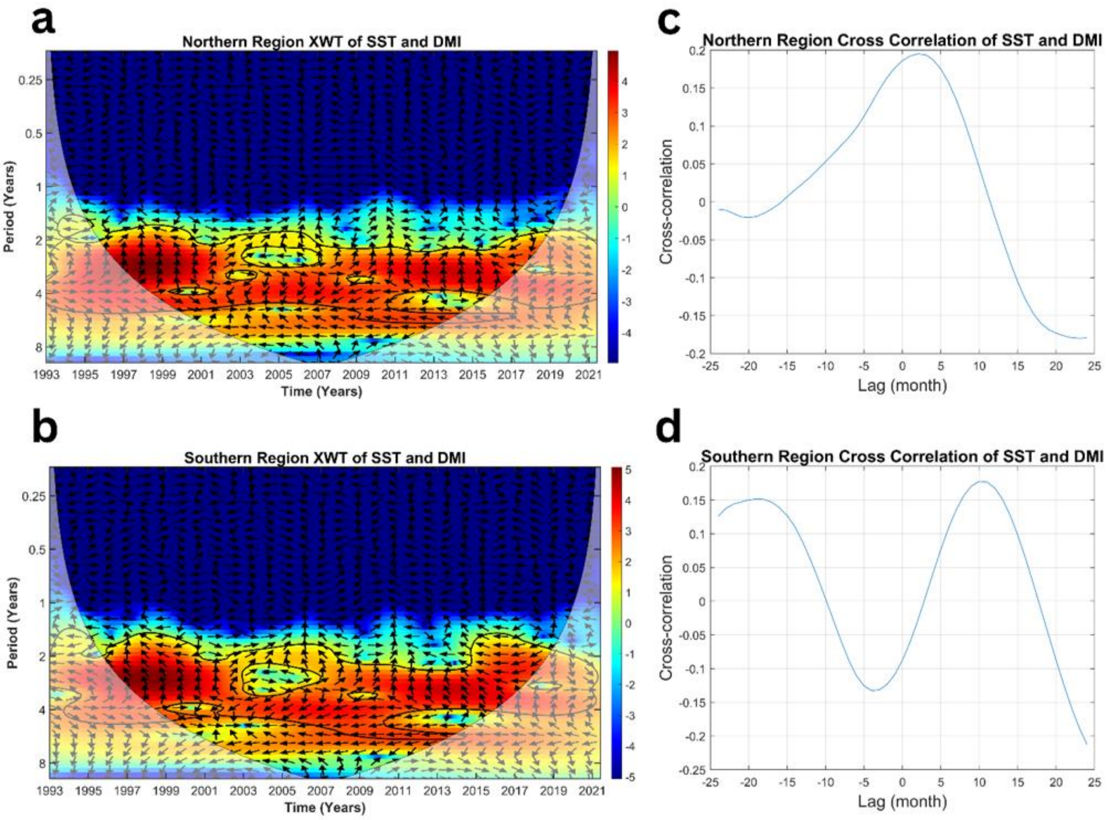

Figure 5. XWT of SST and DMI on Northern Region (a), Southern Region (b) and Cross Correlation of SST and DMI on Northern Region(c) Southern Region(d)

Results show that the IOD has a stronger and more spatially uniform association with SST compared to ENSO. During the El Niño phase, high correlations are observed in the Java Sea (r = 0.6-0.7) and the southern Natuna Sea (r = 0.3-0.5). Conversely, the north of Natuna Sea shows a weaker correlations (r = 0.1-0.3), many of which fall below the significance threshold. In the La Niña phase, although the maximum correlation is lower than that of El Niño, significant links persist in the southerns and central Natuna Sea (r = 0.2 - 0.45) and Java Sea (r = 0.4-0.5).

During the IOD+ phase, the SST-DMI correlation is stronger and significant across almost the whole study area, with peak values in the Java Sea (r > 0.8) and southern natuna Sea (r > 0.7). In contrast, during the IOD- phase, while the correlation remains positive, the correlation value is lower compared to IOD+ phase. Significant correlation in the IOD- phase are primarily concentrated in the Java Sea (r = 0.4 - 0.6) and some parts of the southern Natuna Sea while correlations in the northern Natuna Sea are weaker. All spatial maps show a positive correlation between ENSO/IOD and SST, indicating that increases or decreases in the index correlate with changes in SST.

3.4. Discussion

The spatial analysis of partial correlations shows diverse responses of the Natuna Sea SST to climate variability which aligns with and refines the understanding of regional atmospheric teleconnections. Previous studies have established that ENSO influences remote oceans through an 'atmospheric bridge,' where changes in Walker Circulation modify cloud cover and evaporation, consequently increasing net heat flux into the ocean (Klein et al., 1999; Alexander et al., 2002). This mechanism offers a reasonable explanation for the observed SST variability in the Natuna Sea. The relatively short lag of approximately 2 months identified at Northern Region is consistent with this rapid atmospheric teleconnection. This may suggest that surface heat flux anomalies are likely the dominant factor associating ENSO with warming in the northern region. In contrast, the longer lag observed at Southern Region suggests that this atmospheric signal may be modulated by complex regional circulation and seasonal monsoonal patterns before affecting the southern basin.

Previous research, such as Susilo et al. (2024), Juniarti et al. (2017), and Fathin &

Setiawan (2023), showed a negative relationship between the ENSO/IOD index and SST in the Western Sumatra and Halmahera Seas, which is a contrast to the results in the Natuna Sea. This contrast is highly linked to the semi enclosed geography of the Natuna Sea. Instead of direct oceanic pathways, the climate anomalies are transmitted into this region primarily trough an ‘atmospheric bridge’ mechanism where large scale atmospheric circulation adjustment alter the local air-sea heat fluxes. Consequently, the association between ENSO/IOD and Natuna Sea SST appears to be led through atmospheric pathways rather than direct oceanic advection.

During El Niño, the Indo-western Pacific regional Hadley circulation is weakened, leading to irregular atmosphere descent over the tropical Indo-western Pacific (Klein et al.. 1999, Wang, 2002, 2005, Wang et al., 2006). This process is typically associated with anomalous anticyclones developed in the off equatorial western Pacific, modifying local air temperature, humidity, and cloud distribution over the South China Sea (SCS) (Weisberg and Wang, 1997, Wang et al., 1999, Wang et al., 2006). During the peak phase of El Niño the SCS experiences anomalous descending air movements and a weakening of the Asian Monsoon. This condition leads to a reduced cloud cover and allows the increase of shortwave radiation to warm the sea surface. The strong positive partial correlations identified in Figure 6b support the presence of this warming effect even when IOD signals are removed. Furthermore, the lag analysis helps elaborate the relative importance of these processes. The short lag (2-3 months) at Northern Region is consistent with the rapid radiative heating while the longer lag (7-10 months) at Southern Region suggests that the warming signal might be reinforced or delayed by oceanic advection from the SCS, which requires more time to propagate to the southern region.

There’s an asymmetry intensity of the El Niño and La Niña that occurs in the South China Sea. The South China Sea does not consistently show significant cooling in every La Niña event (Wang et al., 2006, Huang et al., 2013). This asymmetry is reflected in our findings in Figure 6a where the distribution of partial correlation during the La Niña phase is lower in magnitude and lacks a coherent spatial pattern compared to the El Niño phase.

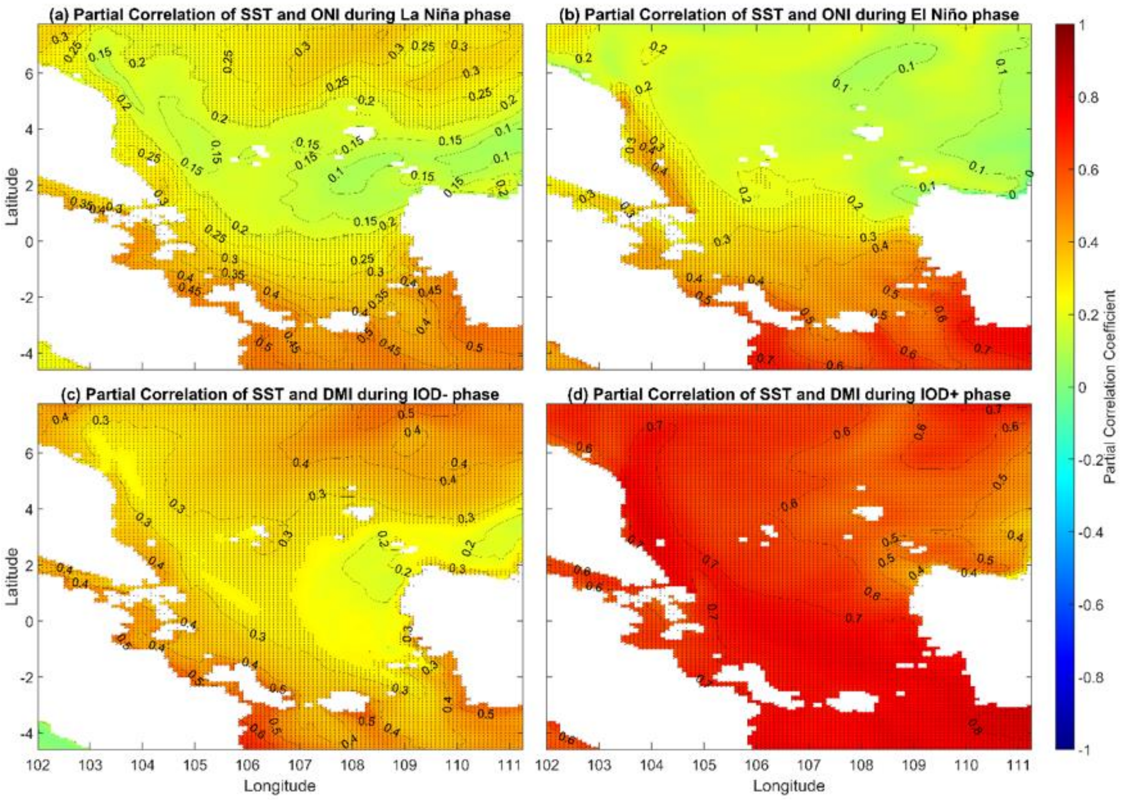

Figure 6. Partial Correlation between SST and ENSO (IOD as control) on La Niña phase (a) El Niño phase (b) Partial Correlation between SST and IOD (ENSO as control) on IOD- phase (c) IOD+ phase (d).

In regard to the IOD. The strong positive correlations observed in this study (figure 6d) are consistent with the hypothesis that IOD modulates SST via surface heat flux alterations (Tanizaki et al., 2017). IOD+ phases are generally associated with less convection and reduced cloud coverage over the Indonesian waters (Rahayu et al., 2018; Fadhloli, 2013). This reduction in cloud cover leads to an increase in solar insolation which likely contributes to the positive SST anomalies observed in the Natuna Sea. Conversely, IOD- phase particularly coincides with enhanced convection and increased cloudiness that consequently block shortwave radiation. While not explicitly analyzed in this study, previous literature also suggests that IOD- phase are linked to heavy precipitation and increased river discharge in Sumatra, Kalimantan, and Java (Ramadhan et al., 2021). It is hypothesized that the influx of cooler freshwater from these rivers may mix with surrounding waters (Yuliardi et al., 2024) and potentially reinforcing the cooling signal (positive correlation) observed during the IOD- phase in figure 6c, particularly in coastal areas.

4. Conclusion

Based on the PSD analysis, SST in the Natuna Sea is characterized by significant interannual oscillations (2-7 years). The spectral peak at 3.28 years shows the important role of interannual timescales fluctuations, where statistical associations with ENSO and IOD contribute more than annual, seasonal, or intraseasonal variations.

The XWT results reveal a diverse spatial heterogeneity in the timing of the SST response. The Northern Region responds rapidly to climate indices with a lag of 2-3 months, while the Southern Region shows a delayed response of 7-10 months. This spatial difference suggests a dual mechanism, the north is consistent with fast atmospheric teleconnections while the delayed signal in the south implied modulation by slower oceanic advection or shelf dynamics.

Partial correlations show a positive relationship between SST and both climate indices, with the IOD demonstrating a stronger and more uniform association than ENSO. During the El Niño phase, correlations range from 0.1 - 0.7 while the La Niña phase shows a weaker and more complex pattern where correlation ranges from 0.1 - 0.6. In contrast, the SST to IOD relationship (with ENSO as control) is notably strong during the IOD+ phase where correlation ranges from 0.5 - 0.8 while the IOD-phase shows a low to moderate correlation ranging from 0.2 - 0.5.

This study indicates that ENSO and IOD are significantly linked to interannual SST in the Natuna Sea. However, the mechanism differs from Indonesian waters that bordering the Pacific or Indian Oceans, which typically show a negative correlation due to direct vertical advection (upwelling). In contrast, the positive correlation observed in the Natuna Sea are consistent with the hypothesis that atmospheric teleconnections via surface heat fluxes are the primary driven in the north. However, as this study relied on statistical associations, future research should explicitly quantify surface heat flux components (latent and sensible heat), wind stress, and ocean current data in order to rigorously verify the relative contributions of atmospheric forcing against oceanic advection.

Acknowledgements

The authors would like to express their gratitude to Tanjungpura University for providing the necessary facilities and support during this research. We extend our thanks to thesis supervisors and examiners for their invaluable assistance in data collection and analysis.

References

Alamsyah, M.Z., Handoyo, G. & Wijaya, Y.J., 2024. Analisis Pengaruh Indian Ocean Dipole Terhadap Suhu Permukaan Laut and Klorofil-a Di Selat Karimata Pada Tahun 2008-2022. Indonesian Journal of Oceanography, 6(3): 257-265. https://doi.org/10.14710/ijoce.v6i3.23635

Alexander, M.A., Bladé, I., Newman, M., et al., 2002. The atmosphericbridge: the influence of ENSO Teleconnections on air-sea Inter-action over the global oceans. J Climate. 15: 2205–2231.

Al-Fiah, L. & Burhanuddin, A., 2023. Pembangunan Keamanan and Inspeksi Maritim di Laut Natuna Utara: masa kini and rekomendasi untuk masa depan. Jurnal Kemaritiman. 4(2):75-84.

Alizadeh, O., 2017. Contrasting global teleconnection features of the eastern Pacific and central Pacific El Niño events. Dynamics of Atmospheres and Oceans. 80: 139-154.

Alizadeh, O., 2022. Amplitude, duration, variability, and seasonal frequency analysis of the El Niño-Southern Oscillation. Climatic Change. 174:201. https://doi.0.1007/s10584-022-03440-w.

Alizadeh, M.R., Abatzoglou, J.T., Adamowski, J.F., Prestemon, J.P., Chittoori, B., Asanjan, A.A. and Sadegh, M., 2022. Increasing Heat-Stress Inequality in a Warming Climate. Earth's Future. https://doi.10.1029/2021EF002488.

Alizadeh, O., 2023. A review of ENSO teleconnections at present and under future global warming. WIREs Climate Change. 15(1): 861.

An, S.I., 2024. A dynamic link between the basin-scale and zonal modes in the tropical Indian Ocean. Theor. Appl. Climatol. 78: 203–215.

Ashok, K., Guan, Z. and Yamagata, T., 2001. Impact of the Indian Ocean Dipole on the relationship between the Indian monsoon rainfall and ENSO. Geophys. Res. Lett. 28: 4499–4502.

Ashok, K., Guan, Z. and Yamagata, T., 2003. Influence of the Indian Ocean Dipole on the Australian winter rainfall. Geophys. Res. Lett. 30: 1821.

Ashok, K., Nakamura, H. and Yamagata, T., 2007. Impacts of ENSO and Indian Ocean Dipole events on the southern hemisphere storm-track activity during Austral winter. J. Clim. 20: 3147–3163.

Belkin, I. M., 2009. Rapid warming of Large Marine Ecosystems. Progress in Oceanography, 81(1-4), 207-213.

Black, E., Slingo, J. and Sperber, K.R., 2003. An observational study of the relationship between excessively strong short rains in coastal East Africa and Indian Ocean SST. Mon. Weather Rev. 131: 74–94.

Cane, M.A., 1983, Oceanographic Events During *El Niño*, Science, 222:1189-1195. DOI:10.1126/science.222.4629.1189

Cai, W. et al., 2014. Increased frequency of extreme Indian Ocean Dipole events due to greenhouse warming. Nature. 510: 254–258.

Clark, C.O., Webster, P.J. and Cole, J.E., 2003. Interdecadal variability of the relationship between the Indian Ocean Zonal Mode and East African coastal rainfall anomalies. J. Clim. 16: 548–554.

Curtis S. and Hastenrath S., 1995. Forcing of anomalous sea surface temperature evolution in the tropical Atlantic during Pacific warmevents. J. Geophys Res. 100: 15835–15847.

Fathin, M.A. and Setiawan, R.Y., 2023. Pengaruh El Niño-Southern Oscillation and Indian Ocean Dipole terhadap Dinamika Klorofil-a and Suhu Permukaan Laut Halmahera. Universitas Gadjah Mada. Thesis.

Grinsted, A. 2024. Cross wavelet and wavelet coherence (https://github.com/grinsted/wavelet-coherence), GitHub. Retrieved December 11, 2024.

Guilford, J.P., 1956. Fundamental Statistics in Psychology and Education (3rd ed.). New York: McGraw-Hill.

Huang, Z., Du, Y., Wu, Y. and Xu, H., 2013. Asymmetric Response of the South China Sea SST to El Niño and La Niña. J. Ocean Univ. China. 12(2): 272-278

Husna, K., Rimawati, S.A. and Sucahyono, D., 2019. Pengaruh Iod (Indian Ocean Dipole) Terhadap Bencana Hidrometeorologi Di Sumatera Utara Periode September Oktober November (SON) 2016. Seminar Nasional Geomatika. 3. 1167.

Fadholi, A., 2013. Studi Dampak El Nino And Indian Ocean Dipole (Iod) Terhadap Curah Hujan Di Pangkalpinang. Jurnal Ilmu Lingkungan, 11(1): 43-50.

Isa, N.S., Akhir, M.F., Kok, P.H., Daud, N.R., Khalil, I. and Roseli, N.H., 2020. Spatial and temporal variability of sea surface temperature during El-Niño Southern Oscillation and Indian Ocean Dipole in the Strait of Malacca and Andaman Sea. Regional Studies in Marine Science. 39: 101402.

Izumo, T. et al., 2010. Influence of the state of the Indian Ocean dipole on the following year's El Niño. Nat. Geosci. 3: 168–172.

Juniarti, L., Jumarang, M.I. and Apriansyah., 2017. Analisis Kondisi Suhu and Salinitas Perairan Barat Sumatera menggunakan Data Argo Float. Physics Communication 1(1): 74-84.

Kertayasa, I.M., Sukarasa, I.K., Widagda, I. and Hendrawan, G., 2013. Pengaruh Indian Ocean Dipole Mode (IODM) Terhadap Intensitas Hujan Di Benua Maritim Indonesia (BMI) BARAT. *Buletin Fisika*, 14(1): 25-30.

Kim, J.W. and An, S.I., 2018. Western North Pacific anticyclone change associated with the El Niño–Indian Ocean Dipole coupling. Int. J. Climatol. 39: 2505-2521.

Klein, S.A., Soden, B. J. and Lau, N.C., 1999. Remote sea surface temperaturevariations during ENSO: evidence for a tropical atmospheric bridge. J Climate. 12: 917-932

Kug, J.S. and Kang, I.S., 2006. Interactive feedback between the Indian Ocean and ENSO. J. Clim. 19: 1784–1801.

Kug, J.S. et al., 2006. Role of the ENSO–Indian Ocean coupling on ENSO variability in a coupled GCM. Geophys. Res. Lett. 33: L09710.

Lanzante J.R., 1996. Lag relationships involving tropical SSTs. J Cli-mate. 9: 2568–2578.

Lareef, A., Rao, A.S. and Yamagata, T., 2003. Modulation of Sri Lankan Maha rainfall by the Indian Ocean Dipole. Geophys. Res. Lett. 30. https://doi.org/10.1029/2002GL015639

Lau N.C. and Nath, M.J., 1996. The role of the atmospheric bridge in linkingtropical Pacific ENSO events to extratropical SST anomalies. JClimate. 9: 2036–2057

Le, T., Ha, K.J., Bae, D.H. and Kim, S.H., 2020. Causal effects of Indian Ocean Dipole on El Niño–Southern Oscillation during 1950–2014 based on high-resolution models and reanalysis data. Environ. Res. Lett. 15: 1040b6.

L'Heureux, M.L., et al., 2017. Version 5 of the Climate Prediction Center Extended Reconstructed Sea Surface Temperature verison 5 (ERSSTv5). Journal of Climate, 30(20): 8179-8205.

Liu, N., Wang, H., Ling, T. and Feng, L., 2013. The Influence of ENSO on Sea Surface Temperature Variations in the China Seas. Acta Oceanologica Sinica. 32(9): 21-29. https://doi.org/10.1007/s13131-013-0348-7

Luo, J.J. et al., 2010. Interaction between El Niño and extreme Indian Ocean dipole. J. Clim. 23: 726–742.

Maharani, W.R., Setiyono, H. and Setyawan, W.B., 2014. Studi Distribusi Suhu, Salinitas And Densitas Secara Vertikal And Horizontal Di Perairan Pesisir, Probolinggo, Jawa Timur. Jurnal Oseanografi. 3(2): 151-160.

NOAA-CPC., 2015. SST Consolidation and El Nino/La Niña Standard Operational Threshold. National Oceanic and Atmospheric Administration, Climate Prediction Center.

Pearson, K., 1895. Contributions to the Mathematical Theory of Evolution. II. Skew Variation in Homogeneous Material. Philosophical Transactions of the Royal Society of London. A. 186: 343–414

Pearson, K., 1900. Mathematical Contributions to the Theory of Evolution. VII. On the Correlation of Characters not Quantitatively Measurable. Philosophical Transactions of the Royal Society of London. Series A. Containing Papers of a Mathematical or Physical Character. 195: 1–47.

Pratama, S. S., Kushadijayanto, A. A. and Risko., 2023. Cycle of Potential Fishing Area of WPP-NRI 711 Year 2011-2020. Jurnal Laut Khatulistiwa. 6(1): 19-29.

Preethi, B., Sabin, T.P., Adedoyin, J.A. and Ashok, K., 2015. Impacts of the ENSO modoki and other tropical Indo-Pacific climate-drivers on African rainfall. Sci. Rep. 5: 16653.

Qadimi. M., Alizadeh. O. and Irannejad, P., 2021. Impacts of the El Niño-Southern Oscillation on the strength and duration of the Indian summer monsoon. Meteorol Atmos Phys. 133: 553–564.

Rahayu, N. D., Sasmito, B. and Bashit, N., 2018. ANALISIS PENGARUH Fenomena Indian Ocean Dipole (IOD) Terhadap Curah Hujan Di Pulau Jawa. Jurnal Geodesi Undip. 7(1): 57-67.

Ramadhan, H., Nugroho, D., Nurjaya, I.W. and Atmadipoera, A.S., 2021. Influence of river discharge on circulation and tidal process in the Java Sea, Indonesia. IOP Conf. Ser. Earth Environ. Sci. 944.

Saji, N.H., Goswami, B.N., Vinayachandran, P.N. and Yamagata, T., 1999. A dipole mode in the tropical Indian Ocean. Nature. 401: 360–363. https://doi.org/10.1038/43854

Saji, N.H. and Yamagata, T., 2003. Possible impacts of Indian Ocean Dipole mode events on global climate. Clim. Res. 25:151–169.

Susilo, A.F.I., Harsono, G. and Wirasatya, A., 2024. Pengaruh IOD (Indian Ocean Dipole) Terhadap Variabilitas Distribusi Suhu Permukaan Laut and Klorofil-a Pada Tahun 2019 di Perairan Meulaboh, Kepulauan Sinabang, Provinsi Aceh. Jurnal Hidrografi Indonesia. 4(2): 57–72.

Tanizaki, C., Tozuka, T., Doi, T. and Yamagata, T., 2017. Relative importance of the processes contributing to the development of SST anomalies in the eastern pole of the Indian Ocean Dipole and its implication for predictability. Climate Dynamics. 49. 10.1007/s00382-016-3382-2.

Tompkins, A.M., 2001. On the Relationship between Tropical Convection and Sea Surface Temperature. *J. Climate*. 14, 633–637.

Torrence C. and Compo G.P., 1998. A practical guide to wavelet analysis. Bull Am Meteorol Soc. 79: 61– 78.

Wang, C., Weisberg, R.H. and Virmani, J.I., 1999. Western Pacific interannual variability associated with the El Niño – Southern Oscillation. J. Geophys. Res. 104: 5131-5149.

Wang, C., 2002. Atmospheric circulation cells associated with the El Niño – Southern Oscillation. J. Clim. 15: 399-419.

Wang, C., 2005. ENSO, Atlantic climate variability, and the Walker and Hadley circulations, in The Hadley Circulation: Past, Present and Future, edited by H. F. Diaz and R. S. Bradley. pp. 173 – 202. Springer. New York.

Wang, C., Wang, W., Wang, D. et al., 2006. Interannual variability of the South China Sea associated with El Niño. J Geophys

Res. 111: C03023.
Wang D., Xie, Q., Du, Y. et al., 2002. The 1997–1998 warm event in the South China Sea. Chinese Sci Bull. 47(14): 1221–1227
Wang, F., Li, X., Tang, X. et al., 2023. The seas around China in a warming climate. Nature Reviews Earth & Environment, 4: 535–551.
Webster, P.J., Moore, A.M., Loschnigg, J.P. and Leben, R.R., 1999. Coupled Ocean-atmosphere dynamics in the Indian Ocean during 1997–98. Nature. 401: 356-360.
Weisberg, R. H. and Wang, C., 1997. A western Pacific oscillator paradigm for the El Niño – Southern Oscillation. Geophys. Res. Lett. 24: 779-782.
Xie, S.P., Xie, Q., Wang, D. et al., 2003, Summer up-welling in the South China Sea and its role in regional climatevariations. J Geophys Res. 108(C8): 3261
Yuliardi, A.Y., Rachman, H.A., Sari, R.J., Rahmalia, D.A., Nugroho, A.T. and Prayogo, L.M., 2024. Analisis Variasi Musiman Suhu, Salinitas, and Arus Permukaan di Perairan Madura. Indonesian Journal of Oceanography. 6(4): 292-305.
Zhu, X., Wang, W., Zhou, W. et al., 2003. Interannual mode of sea surfacetemperature in relation to monsoon forcing in South China Sea. J Tropical Oceanogr. 22(4): 42–50.

Copyright: © 2025 by authors. Licensed Fisheries and Marine Science Faculty, Jenderal Soedirman University. This article is licensed under a Creative Commons Attribution 4.0 International License (CC BY). It permits to share and to adapt as long as appropriate credit to the original author(s) and source is provided (https://creativecommons.org/licenses/by/4.0/).